Universidad Industrial de Santander

Dimer structure as topological pinning center in a superconducting sample
Dados como centro de anclaje topológico en una muestra superconductora

Cristian A. Aguirre[1], Miryam R. Joya[2a], J. Barba-Ortega[2b, 3]

[1]Departamento de Física, Universidad Federal de Mato Grosso, Cuiabá, Brasil. Email: cristian@fisica.ufmt.br
[2] Departamento de Física, Universidad Nacional de Colombia, Bogotá, Colombia. Orcid: [a] 0000-0003-3415-1811.
Emails: [a] mrinconj@unal.edu.co, [b] jjbarbao@unal.edu.co
[3]Foundation of Researchers in Science and Technology of Materials (Foristom), Colombia.

Abstract

Solving the Ginzburg-Landau equations, we analyzed the vortex matter in a superconducting square with a Dimer structure of circular pinning centers generated by a pulsed heat source in the presence of an applied magnetic field. We numerically solved the Ginzburg-Landau equations in order to describe the effect of the temperature of the circular defects on the Abrikosov state of the sample. The pulsed laser produced a variation of the temperature in each defect. It is shown that an anomalous vortex-anti-vortex state (A-aV) appears spontaneously at higher magnetic fields. This could be due to the breaking of the symmetry of the sample by the inclusion of the thermal defects.

Keywords: Ginzburg-Landau; mesoscopic; magnetization; vortices.

Resumen

Resolviendo las ecuaciones de Ginzburg-Landau, analizamos el estado de vórtice en un cuadrado superconductor con centros de anclaje circulares en forma de una estructura de Dados, generados por una fuente de calor pulsada y en presencia de un campo magnético aplicado. Resolvimos numéricamente las ecuaciones Ginzburg-Landau para describir el efecto de la temperatura de los defectos sobre el estado Abrikosov de la muestra. El láser pulsado produce una variación de la temperatura en cada defecto. Se muestra que un estado anómalo vórtice-anti-vórtice (A-aV), aparece espontáneamente hacia campos magnéticos altos. Esto podría deberse a la ruptura de la simetría de la muestra por la inclusión de los defectos térmicos.

Palabras clave: Ginzburg-Landau; mesoscópico; magnetización; vórtices.

1. Introduction

Over the last few decades, due to advances in technology, many theoretical and experimental investigations have shown that pinning and anti-pinning array centers (dots or anti-dots) enhance the critical parameters of low-temperature superconducting materials [1, 2, 3, 4, 5, 9, 10, 11].

Historically, several kinds of lasers have been used, such as the yttrium-aluminium-garnet, Ruby, free electron, and semiconductor types, among others. As is well known, a laser is concentrated light radiation of a quasi-

single monochromatic wavelength, which depends on the active medium used for its generation. The technology of the fabrication of pinning centers with a laser is based on the timely concentration of light on the surface of the sample, producing an increase in temperature on the surface of the material [6, 7, 8].

Topological centers can be produced by several physical and chemical methods [12, 13, 14]. Several investigations have been carried out on defects within a Dimer lattice. For example, A. He et al. studied the degeneracy of the Abrikosov matter in a Dimer network of anti-dots with the Ginzburg-Landau model. They found interesting vortex configurations and demonstrated that certain vortex states can be determined by local constraints [15].

V. Kapaklis et al. proposed spin ice configurations in order to analyze monopole-like magnetic excitations, finding dynamic effects [16]. A. Farhan et al. directly visualized the creation of a magnetic charge in a bi-dimensional spin ice system. They found a temperature dependence of screened magnetic charge defects [17]. S. Korshunov investigated the structure of the ground state of an XY model in a Dimer-lattice configuration, the results constituting a tool applicable to the study of Josephson junctions in an external magnetic field [18]. C. Xue experimentally studied Shubnikov matter in a Kagome structure of elliptical anti-dots. They found that the vortex patterns are very close to those found by solving the GLE [19, 20].

On the subject of non-conventional vortex-anti-vortex generation pairs, one of the authors of the present paper theoretically investigated superconducting matter in a bidimensional square with a square defect. The results showed that the vorticity decreases when the applied magnetic field is increased, due to the symmetry breaking in this sample [21]. Kosterlitz et al. predicted that vortexanti-vortex pairs dissociate into free fluxoids in neutral superfluids [22, 23]. Misko et al. found a thermodynamically stable vortex-anti-vortex pattern in mesoscopic triangles due to the change of sign of the vortex-vortex and vortex-anti-vortex interaction forces [24].

In the present paper, we used the GL model to analyze the magnetic moment density and Abrikosov-Shubnikov matter of a superconducting square immersed in an applied external magnetic field. We considered a Dimer structure of pairs of circular defects with different temperatures in the sample.

This Dimer landscape is produced by a laser that emits light coherently at chosen points on the material. The laser produces pulses of light, making possible the fabrication of this structure in the superconducting sample. We found a non-conventional vortex-anti-vortex configuration under a high magnetic field for one studied case.

2. Theoretical formalism

We considered a thin slab of a superconducting square with thickness $d = 0,1\xi, d << \xi$ with circular pairs of pinning centers at temperatures T_e and T_i and radius r. The time-dependent Ginzburg-Landau equations in dimensionless units for the pseudo-function ψ and the vector potential $\mathbf{A}$ are given by [25, 26, 27, 28, 29, 30]:

$$\frac{\partial \psi}{\partial t} = -(i\nabla + \mathbf{A})^2 \psi + (1 - T(x, y))\psi (1 - |\psi|^2) \quad (1)$$

$$\frac{\partial \psi}{\partial t} = (1 - T(x, y))Re[\bar{\psi}(-i\nabla - \mathbf{A}) \psi] - \kappa^2 \nabla \times \nabla \times \mathbf{A} \quad (2)$$

We take the usual superconducting-vacuum interface idealized by: $\mathbf{n} \cdot (i\nabla + \mathbf{A})\psi = \mathbf{0}$ [31, 32]. The equations 1 and 2 are in dimensionless units, as follows: ψ in units of $\psi\infty = \sqrt{-\alpha}/\beta$, where α and β are two adimensional phenomenological parameters, lengths in units of the coherence length $\xi = \hbar/\sqrt{-4m\alpha_0}$; time in units of $t_0 = \pi\hbar/8K_BT_c$; and $\mathbf{A}$ in units of $H_{c2}\xi$, where $H_{c2} = c\hbar /2e\xi^2 = \kappa \sqrt{2H_c}$; is the upper critical field. The function $T(x, y)$ provides the regions where $T = T_e$ and $T = T_i$ are used. $\kappa = \lambda/\xi = 1,3$ is the typical Ginzburg-Landau parameter value for an Al alloy [33, 34], with mean free path $\sim 1\mu m$, $\lambda = c \sqrt{m^*\pi} /2e^*\psi$ is the magnetic field penetration depth.

3. Results and discussion

We analyzed a superconducting flat square with area $L \times L = 30 \times 30$. The radius of the circular internal defects was $r = 1\xi$. T_e and T_i are the temperatures of the external and internal circular defects, respectively. The size of the grid $\delta_x = \delta_y = 0,1$. We take $T = 0,2$ for all samples (see Figure 1(a)) where the layout of a possible experimental setup of the studied sample immersed in a magnetic field H. In the Figure 1(b), we plot the studied sample of $L = 30$, (and the Figure 1(c) $L = 60$). The Dimerstructure made of two circular defects with radius $r = 1\xi$ at temperatures (external defect) $T_e > T$ and (internal defect) $T_i > T$ is shown in the Figure 1(d). We considered the three following scenarios:

- Case 1: $T_e = 0,4$ and $T_i = 0,8$
- Case 2: $T_e = 0,8$ and $T_i = 0,4$
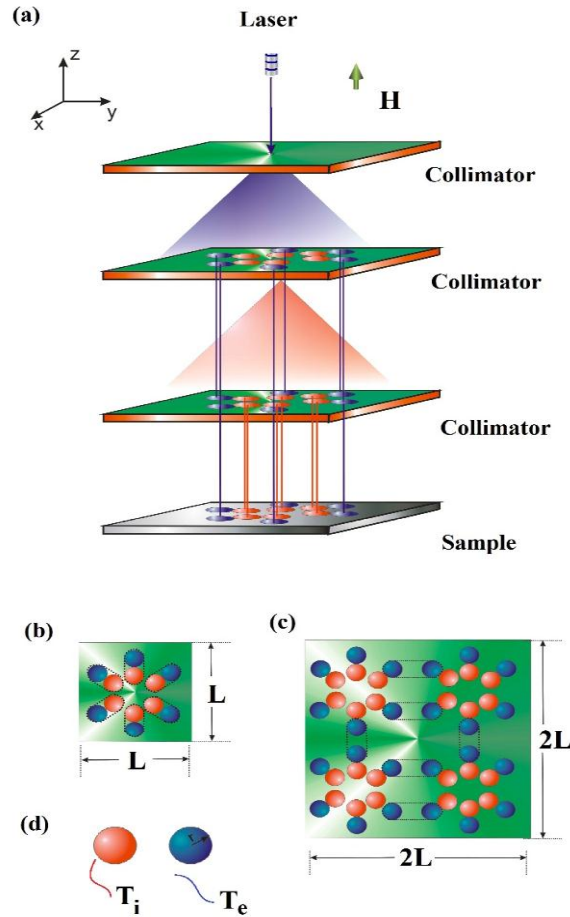- Case 3: $T_e = 0,8$ and $T_i = 0,8$

Figure 1: (a) Layout of a possible experimental setup of the studied sample immersed in a magnetic field H at $T = 0{,}2$ by using a laser light at the far field passing through a metallic mask to create spatially modulated depletion of the superconducting condensate. Superconducting square of side (b) $L = 30$ ((c) $L = 60$) with a Dimer-structure made of two circular defects with radius $r = 1\xi$ at (d) temperatures (external defect) $T_e > T$ and (internal defect) $T_i > T$.

With these considerations, in Figure 2 (a), the vorticity N or number of fluxoids, and (b) the magnetization $-4\pi M$ as a function of H for the three indicated cases are plotted. As we can see, the vorticity increases with H, as is usual in a mesoscopic superconductor. On increasing H, more vortices enter the sample when the temperature of the external defect is higher (T_e). However, a nonconventional behavior can be seen in the vorticity for case 3, a transition from $N = 40$ at $H = 0{,}90$ to $N = 32$ at $H = 0{,}91$. (See Figure 2). In Figure 3(a-d), the magnetic induction $\mathbf{B}$ for the indicated values of H for the studied cases is shown. All panels are the frontal view of the magnetic induction at $z = 0$ and $(x, L/2)$. As expected, in all the figures we observed an increase in the number of oscillations in the zone $(x; L/2, 0)$ when the vorticity N increases. In Figure 3 (a), for case 1, we found 1, 4, and 6 oscillations for $N = 6$, 22, and 38 at $H = 0{,}890$, 0,908, and 0,920, respectively. It is interesting to note that for case 1, the amplitude of the oscillations is constant.

This means that in all the zx planes there is the same number of vortices N. This situation does not occur in cases 2 and 3. Given that in case 3 both defects exhibit temperatures near T_c, the Debye energy window is smaller than in cases 1 and 2.

In terms of the energy, the probability of the appearance of anti-vortices increases with the arrival at the limit, where the mediation of the network and the interaction between the vortices exhibits a coherent phase. In Figure 3 (b) for cases 1 and 2, we see $N = 6$, 6, and 26 at $H = 0{,}890$, 0,836, and 0,848, 1, 1, and 5 oscillations with different amplitudes, respectively. Finally, in Figure 3 (c), we can see for $N = 20$, 28, and 40 at $H = 0{,}880$, 0,886, and 0,900, 3, 6, and 6 oscillations, and $N = 32$, 26, 20 at $H = 0{,}910$, 0,916, and 0,924, with 6 oscillations, independent of N (Figures 3 (d)).
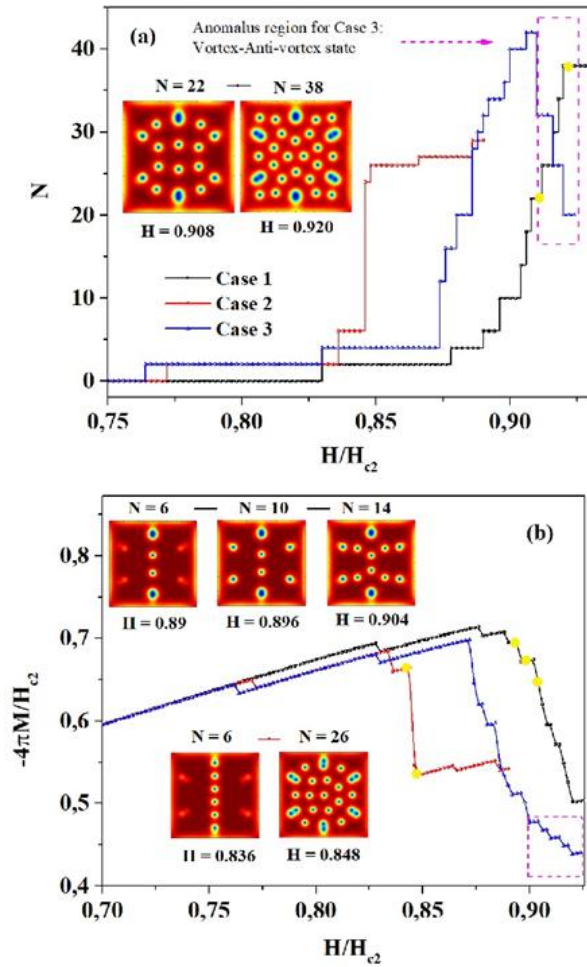
Figure 2. (Color online) (a) Vorticity N , (b) Magnetization −4πM and as a function of *H* for a Dimer structure for the studied cases. (Inset) superconducting electronic density $|\psi|^2$ at indicated *H*.

In this last figure, it can be seen that *B* increases with *H*, so the possible anti-vortex states do not appear in the central region of the sample. In Figure 4, the density of the Cooper pairs and the Δφ phase difference can be seen for the indicated *H*. The vortices enter the sample by the close regions to the defects with a higher temperature.

Furthermore, due to the effects of the proximity, and the possible anharmonic vibrations in the network, there are regions where the vortices overlap. Although these vibrations are anharmonic, the superposition of the two vibrations doesn't cause a departure from coherent phase (Debye energy), which allows the appearance of huge vortices to be possible, even when they have different phases and energies.
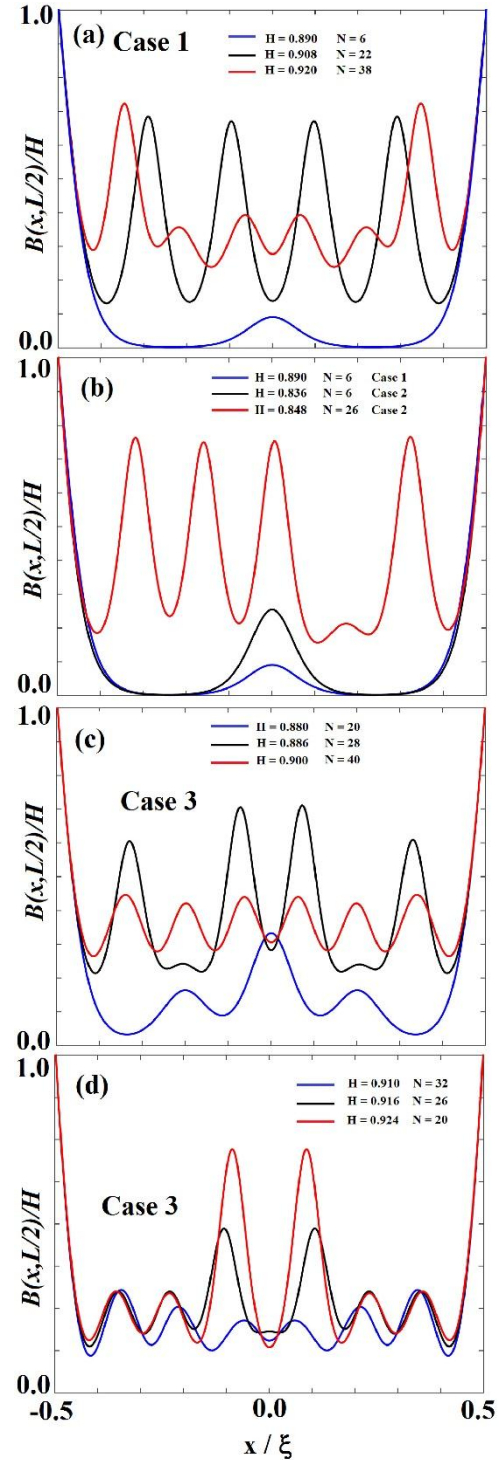

Figure 3. (Color online) (a-d) Magnetic induction *B* for indicated *H* and cases. All panels are the frontal view of magnetic induction in $\chi = 0$ and (*x*, *L*/2).

In Figures 4 and 5, we plot (a) the square modulus of the order parameter $|\psi|^2$, and (b) its Δφ phase, at the *H* fields indicated for case 3. In all the cases studied, the vortices

enter the sample through the sides, with defects closer to its edges. This behavior is to be expected, with a stationary vortex state with $N = 2, 4, 12, 16, 20$, and 28 at $H = 0,764, 0,830, 0,874, 0,876, 0,880$, and $0,886$, respectively (Figure 4). As is well known, the vortices generate a local interaction between the more distant ones, in turn, there is confinement exhibited because of the effects of the proximity between the vortices. This causes, in the vicinities, the inclusion of vortices to need greater energy in order to break the superconductor pairing.
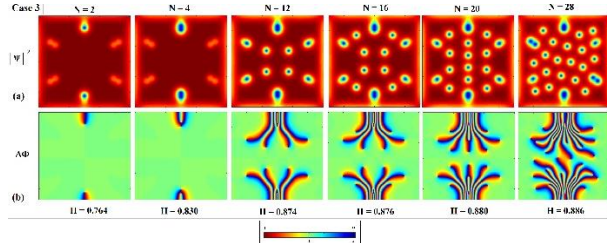

Figure 4. (Color online) (a) Order parameter $|\psi|^2$ and (b) its phase $\Delta\varphi$ for determinate H, for the case 3. $\psi \simeq 0$ (normal state - blue zones) and $\psi \simeq 1$ (superconducting state - red zones). From blue to red zones represent $\Delta\varphi$ from $-\pi$ to π.
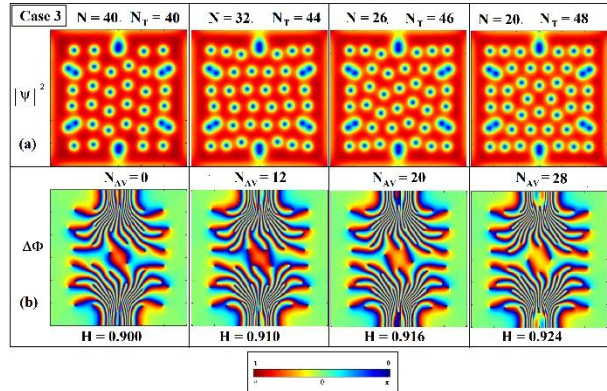

Figure 5. (Color online) (a) Order parameter $|\psi|^2$, and (b) its phase $\Delta\varphi$, at indicated H for case 3. N is the vortex number, N_{AV} is the number of anti-vortices, and N_T is the total vorticity, so $N_T = N + N_{AV}$. $\psi \simeq 0$ (normal state) and $\psi \simeq 1$ (superconducting state). From blue to red regions represent $\Delta\varphi$ from $-\pi$ to π

In Figure 5, we can see a traditional behavior, with the total vorticity $N_T = 40, 44, 46$, and 48 at $H = 0,900, 0,910, 0,916$, and $0,924$ (N increases with increasing H). But if the number of vortices plus the number of anti-vortices is calculated, we see $N = 40, 32, 26$, and 20 (see Figure 2(a) in the anomalous region), and a decrease of the net magnetic flux can be seen. An appreciable decrease of the net quantized magnetic flux is found. Unfortunately,

an anti-vortex is not visible in the $|\psi|^2$ graph, but on carefully observing the phase of the order parameter $\Delta\varphi$ (Figure 5(b)), and knowing that the circulation is in a closed path from blue to red regions, representing changes of the phase from $-\pi$ to π, indicating the presence of a $N = 1$ vortex, changes of the phase from π to $-\pi$ would indicate a presence of a $N = -1$ anti-vortex. A possible explanation for this fact could be a spontaneous generation of anti-vortex states due to possible oscillations in different normal modes in the network, with $N_{AV} = 12, 20$, and 28 anti-vortices, respectively [21].

In Figure 6, we show (a) $|\psi|^2$, (b) its phase $\Delta\varphi$, and (c) the supercurrent J at the indicated H. For case 3, for a sample $L = 60\xi$, stationary vortex states with $N = 4, 8, 32$, and 40 at $H = 0,764, 0,830, 0,874, 0,882$, and $0,892$ can be seen. The super-current J exhibits circulation in the direction opposite from the Meissner current, as is well known.
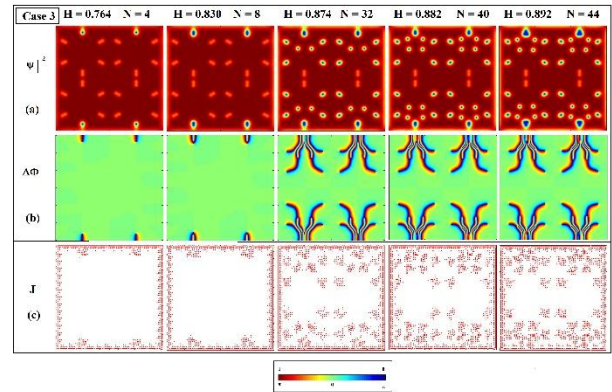

Figure 6: (Color online) (a) Order parameter $|\psi|^2$, (b) its phase $\Delta\varphi$, and (c) the supercurrent J at indicated H for the case 3, for $L = 60\xi$. $\psi \simeq 0$ (normal state) and $\psi \simeq 1$ (superconducting state). From blue to red zones represent $\Delta\varphi$ from $-\pi$ to π.

4. Conclusions

We show how to generate a Dimer-type network at different local temperatures by directing laser pulses at a meso-square superconductor. We also show how an anomalous vortex state decreases as the magnetic field increases. Its behavior is generated under strong fields when both pairs of circular defects are considered with the same temperature $T = 0,8$. We try to explain this phenomenon by including a spontaneous generation of vortexanti-vortex states due to the Dimer structure of the system. Furthermore, we show that the coherent behavior of the optical phonons, which takes into account the anharmonic oscillations of the crystal network, causes the appearance of anti-vortices, given a smaller Debye

window. The magnetic field at the first vortex pairâs entry occurs in sample H_1, and depends on the local temperature of the defects generated by this pulse. H_1 increases as T_e increases, diminishing the surface energy barrier. Additionally, we show the behavior of $\Delta\varphi$, $|\psi|^2$, and the magnetic induction B for the Dimer configuration, showing that if the field is strong, so is the central attenuation.

Acknowledgements

References

[1] G. R. Berdiyorov M. V. Milošević and F. M. Peeters, "Novel Commensurability Effects in Superconducting Films with Antidot Arrays," *Phys. Rev. Lett.*, no. 96, p. 207001,207004, 2006.

[2] A. S. Melnikov, I. M. Nefedov, D. A. Ryzhov, I. A. Shereshevskii, V. M. Vinokur, and P. P. Vysheslavtsev, "Vortex states and magnetization curve of square mesoscopic superconductors," *Phys. Rev. B*, no. 65(R), pp. 140501-140503,140503-140504, 2002.

[3] R. Geurts M. V. Milošević and F. M. Peeters, "Symmetric and Asymmetric Vortex-Antivortex Molecules in a Fourfold Superconducting Geometry," *Phys. Rev. Lett.*, no. 97, pp. 137001-137002,137002-137004, 2006.

[4] E. S. J. Barba-Ortega and J. A. Aguiar, "Superconducting boundary conditions for mesoscopic circular samples," *Supercond. Sci. Technol.*, no. 24, pp. 15001,15001-15007, 2011.

[5] B. Maiorov, S. A. Baily, H. Zhou, O. Ugurlu, J. A. Kennison, P. C. Dowden, T. G. Holesinger, S. R. Foltyn, and L. Civale, "To use or not to use cool superconductors?," *Nat. Matter*, vol. 8, p. 398,404, 2009.

[6] W. T. Silfvast, *Laser Fundamentals*. Cambridge: Cambridge University Press, 2004.

[7] M. Csele, *Fundamentals of Light Sources and Lasers*. New Jersey: John Wiley and Sons, 2011.

[8] M. Allmen and A. Blatter, *Laser-Beam Interactions with Materials: Physical Principles and Applications*. Berlin, Heidelberg: Springer Series in Materials Science, 2013.

[9] Alexey V. Ovcharov, Pavel N. Degtyarenko, Vsevolod N. Chepikov, Alexander L. Vasiliev, Sergey Yu. Gavrilkin, Igor A. Karateev, Alexey Yu. Tsvetkov and Andrey R. Kaul, "Microstructure and superconducting properties of high-rate PLD-derived GdBa_2Cu_3O_{7-δ} coated conductors with BaSnO_3 and BaZrO_3 pinning centers," *Sci. Rep.*, vol. 9, pp. 15231-15235,15235-15237, 2019.

[10] L. Ceccarelli, D. Vasyukov, M. Wyss, G. Romagnoli, N. Rossi, L. Moser, and M. Poggio, "Imaging pinning and expulsion of individual superconducting vortices in amorphous MoSi thin films," *Phys. Rev. B*, vol. 100, pp. 104501-104504,104504-104509, 2019.

[11] M. T. Li,Y. F. Fang, Z. Sun. J. C. Zhang, and C. T. Lin, "Evidence for weak collective pinning and δl pinning in topological superconductor Cu_xBi_2Se_3," *J. Phys. Condens. Matter*, vol. 100, pp. 104501-104504,104504-104509, 2018.

[12] J. L. MacManus-Driscoll, S. R. Foltyn, Q. X. Jia, H. Wang, A. Serquis, L. Civale, B. Maiorov, M. E. Hawley, M. P. Maley, D. E. Peterson, "Strongly enhanced current densities in superconducting coated conductors of YBa_2Cu_3O_{7-x} + BaZrO_3," *Nat. Matter*, vol. 3, p. 439,443, 2004.

[13] R. B. G. Kramer, A. V. Silhanek, W. Gillijns, V. V. Moshchalkov, "Imaging the Statics and Dynamics of Superconducting Vortices and Antivortices Induced by Magnetic Microdisks," *Phys. Rev. X*, no. 1, pp. 21001-21004,21004-21007, 2011.

[14] J. S. León M. R. Joya and J. Barba-Ortega, "IKagome–Honeycomb structure produced using a wave laser in a T conventional superconductor," *Optik (Stuttg).*, no. 172, p. 311,316, 2018.

[15] A. He C. Xue and Y.-H. Zhou, "The ice-like vortex states in a nanostructured superconducting film with a dice lattice of elongated antidots," *AIP Adv.*, no. 8, pp. 85201-85208,85208, 2018.

[16] V. Kapaklis, U. B. Arnalds, A. Farhan, R. V. Chopdekar, A. Balan, A. Scholl, L. J. Heyderman, and B. Hjorrvarsson, "Thermal fluctuations in artificial spin ice," *Nat. Commun.*, vol. 9, pp. 514–519, 2014.

[17] A. Farhan, A . Scholl, C. F. Petersen, L. Anghinolfi, C. Wuth, S. Dhuey, R. V. Chopdekar, P. Mellado, M. J. Alava, and S. Dijken, "Thermodynamics of emergent magnetic charge screening in artificial spin

ice," *Nat. Commun.*, vol. 7, pp. 12631-12635,12635-12636, 2016.

[18]   S. E. Korshunov, "Vortex ordering in fully frustrated superconducting systems with a dice lattice," *Phys. Rev. B*, no. 63, pp. 134501-134503,134503-134505, 2001.

[19]   C. Xue, J. Y. Ge, A. He, V. S. Zharinov, V. V. Moshchalkov, Y. H. Zhou, A. V. Silhanek, and J. Van de Vondel, "Tunable artificial vortex ice in nanostructured superconductors with a frustrated kagome lattice of paired antidots," *Phys. Rev. B*, no. 97, pp. 134501-134506,134506-134507, 2018.

[20]   C. Xue, J. Y. Ge, A. He, V. S. Zharinov, V. V. Moshchalkov, Y. H. Zhou, A. V. Silhanek, and J. Van de Vondel, "Mapping degenerate vortex states in a kagome lattice of elongated antidots via scanning Hall probe microscopy," *Phys. Rev. B*, no. 96, pp. 24510-24511,24510-24516, 2017.

[21]   J. Barba-Ortega, J. L. Aguilar, and J. D. González, "Unconventional anti-vortex spontaneous generation in a superconducting microstructure," *Mod. Phys. Lett. B*, vol. 29, no. 14, p. 1550070, May 2015.

[22]   J. M. Kosterlitz and D. J. Thouless, "Ordering, metastability and phase transitions in two-dimensional systems," *J. Phys. C*, no. 6, p. 1181,1203, 1973.

[23]   D. J. Bishop and J. Reppy, "Study of the Superfluid Transition in Two-Dimensional 4He Films," *Phys. Rev. Lett.*, no. 40 (1727), p. 5171,5185, 1978.

[24]   V. R. Misko, V. M. Fomin, J. T. Devreese and V. V. Moshchalkov, "Stable Vortex-Antivortex Molecules in Mesoscopic Superconducting Triangles," *Phys. Rev. Lett.*, no. 90, pp. 147001-147003,147003-147004, 2003.

[25]   A. Andronov, I. Gordion, V. Kurin, I. Nefedov, and I. Shereshevsky, "Kinematic vortices and phase slip lines in the dynamics of the resistive state of narrow superconductive thin film channels," *Phys. C*, no. 213, p. 193,199, 1993.

[26]   L. Kramer and R. J. Watts-Tobin, "Theory of Dissipative Current-Carrying States in Superconducting Filaments," *Phys. Rev. Lett.*, no. 40, p. 1041,1044, 1978.

[27]   J. Watts-Tobin, Y. Krähenbühl, and L. Kramer, "Nonequilibrium theory of dirty, current-carrying superconductors: phase-slip oscillators in narrow filaments near T_c," *J. Low Temp. Phys.*, no. 42, pp. 459–501, 1981.

[28]   D. Y. Vodolazov, F. M. Peeters, M. Morelle, and V. V. Moshchalkov, "Masking effect of heat dissipation on the current-voltage characteristics of a mesoscopic superconducting sample with leads," *Physical Review B*, no. 71, pp. 184502-1,184502-8, 2005

[29]   M. V. Milošević and R. Geurts, "The Ginzburg–Landau theory in application," *Phys. C Supercond.*, vol. 470, no. 19, pp. 791–795, Oct. 2010.

[30]   C. A. Aguirre, Q. Martins and J. Barba-Ortega, "Desarrollo analítico de las ecuaciones Ginzburg-Landau para películas delgadas superconductoras en presencia de corrientes," *Rev. UIS Ing.*, no. 18(2), p. 213,220, 2019.

[31]   W. D. Gropp, H. G. Kaper, G. K. Leaf, D. M. Levine, M. Palumbo and V. M. Vinokur," *J. Comuptational Physcis*, no. 123, p. 254,266, 1996.

[32]   G. C. Buscaglia, C. Bolech and A. Lopez, *Connectivity and Superconductivity*. J. Rubinstein, Heidelberg: Springer, 2000.

[33]   C. Buscaglia and A. Lopez, *Nanoscience and Engineering in Superconductivity*. Eds V. V. Moshchalkov, R. Woerdenweber and W. Lang, Springer, 2010.

[34]   C. P. Jr, *Handbook of Superconductivity*. San Diego, USA: Academic Press, 2000.